Chapter 2
Longitudinal Relaxation in Solid ^{129}Xe

As if that blind rage had washed me clean, rid me of hope; for the first time, in that gentle indifference of the world. Finding it so much like myself—so like a brother, really—I felt that I had been happy and that I was happy again.
— The Stranger, Albert Camus

2.1 Introduction

Solid xenon has been studied for many years by many prolific groups. The problem of longitudinal relaxation of solid ^{129}Xe in particular is an interesting one because it is notoriously difficult: computationally due to its many-body nature, and experimentally because of its history of nonreproducibility. The wave function of a xenon atom in a lattice is not completely known because of the complexity of the system. In theory, if a correct xenon wave function is used and the correct relaxation mechanism is posited, the relaxation rates are calculable from first principles. At the time of this work, the leading model gives that longitudinal relaxation in the regime of 77–120 K is predominately caused by a spin-rotation interaction mediated by Raman-scattering of phonons. As presented in the literature, this model does not account for our experimental longitudinal relaxation data, and, minimally, requires adjustment to the interaction strength in order for experimental agreement to occur. An overview of the previous theoretical model and experimental data is given in Sect. 2.2.

The measurements in Sect. 2.4 have an unprecedented precision and reproducibility of solid ^{129}Xe longitudinal relaxation times T_1. So-called "snow" and "ice" forms of solid xenon are measured, where an unexpected difference in T_1 times is found. Temperature-dependent T_1 data for ice and snow are also given and compared to predicted relaxation times. The ice data are found to give consistently longer T_1 times across the range of validity of the theory.

Practically, this work may have ramifications for the cyrogenic storage of hyperpolarized xenon. In particular, flow-through xenon polarizers for lung imaging use cryogenic separation and collection of xenon, after which the xenon is transported, revolatilized, and administered to patients. If, perhaps, there are better ways to make the solid (i.e., significantly lengthen T_1) than the methods currently being used, it is an avenue worth exploring.

M. E. Limes, ^{129}*Xe Relaxation and Rabi Oscillations,* Springer Theses,
DOI 10.1007/978-3-319-13632-5_2

2.2 History of the Problem

Previous to experiment, it was assumed that solid ^{129}Xe would have extremely long longitudinal relaxation times limited by direct-dipolar interactions between the spin-1/2 nuclei. Unfortunately for the field of hyperpolarized noble gases, the measured longitudinal relaxation times were significantly shorter than expected (hours instead of months) at 77 K. Because of these unexpectedly short times, there was a need to understand the mechanism of relaxation in this system.

In the following sections, a brief history of theoretical and experimental results is presented as a companion for a reader delving through the literature. As such, notational changes are abundant but clearly labeled after each equation. Section 2.2.1 discusses the history of the theory in conjunction with the history of the experiments. Then, a discussion of more recent experimental results is given in Sect. 2.2.2, followed by a detailed explanation of the theory of the spin-rotation interaction mediated by Raman-scattering of phonons.

2.2.1 Foundations of Theory and Experiment

The spin-rotation interaction is originally proposed to account for gaseous ^{129}Xe longitudinal relaxation by Adrian in his thesis work, where he deemed the mechanism too weak to cause the relaxation [61]. In 1963, Torrey reconsiders and popularizes the idea of the spin-rotation interaction to describe experimental relaxation times of gaseous and liquid ^{129}Xe [62] that are observed by Streever, Hunt, and Carr [63, 64]. These papers serve to rule out the direct-dipolar interaction between nuclei (using the method of Bloembergen, Purcell, and Pound [65]) to account for the relaxation mechanism in liquid ^{129}Xe. Torrey claims that Adrian's chosen method of approximation for a certain summation (that arises from Wick's theory [66], determining a magnetic field at a nucleus of a diatomic molecule produced by molecular rotation) is too crude, and provides an alternative way to evaluate the chemical shift. Both Adrian and Torrey adapt a methodology presented in Ramsey's seminal paper on chemical shifts [49].

In Ramsey's 1950 calculation, a second-order perturbation theory is used to calculate an average-magnetic-shielding constant for each nucleus that describes frequency shifts in an NMR experiment. The assumptions made are: (1) the nuclei of the molecules are so massive compared to the electrons that the nuclei are classical and stationary, (2) the electron spin can be omitted, (3) only one nucleus in the molecule has a nonzero magnetic moment that is in the same direction as the externally applied field, and (4) there is no preferred direction for the molecules, so an average over all orientations is required. The equation for the average-magnetic-shielding constant (Eq. 10 in Ramsey [49]) is computationally impractical for a general molecule because the equation includes a summation over all excited states of the molecule. However, Ramsey shows that it is possible to relate the difficult summation to

an experimentally measurable spin-rotational, magnetic-interaction constant. Using perturbation theory, Ramsey derives an equation for the average-magnetic-shielding constant for a $^1\Sigma$ linear (diatomic) molecule,

$$\sigma = (e^2/3mc^2)\left[\langle 0|\sum_k 1/r_k|0\rangle - (1/ec\omega)(H_r - Ze\omega/cR)\right], \tag{2.1}$$

where e is the electron charge, m is the electron mass, c is the speed of light, r_k is the distance of the kth electron from the nucleus for which the shift is being calculated, ω is the angular velocity about the center of mass, H_r is the magnetic field at that nucleus due to rotation of the diatomic system, Z is the atomic number, and R is the internuclear separation of the pair. Ramsey also elegantly shows Eq. 2.1 is obtained without using second-order perturbation theory, but with sheer physical reasoning.

Torrey bases his 1963 paper on Eq. 2.1 [62]. Torrey's calculation yields the difference in average-magnetic-shielding constants for a xenon diatomic molecule from that of a bare xenon atom ($\Delta\sigma_{\text{av}} = \sigma_{\text{diatomic}} - \sigma_{\text{bare}}$). In comparison to Hunt and Carr's experimental results [64], this calculation is too small by one order of magnitude. This discrepancy translates to an inaccurate magnetic field calculated at the nuclei in question. Nevertheless, Torrey states that there is little doubt the mechanism is spin-rotation. Shown in Torrey [62] is a rigid-sphere calculation which leads to a conglomeration of the longitudinal relaxation time and the difference in average magnetic shielding constants that is similar to experimental results,

$$\begin{aligned}\left[T_1(\langle\Delta\sigma\rangle_{\text{av(Torrey)}})^2\right]_{\text{Torrey}} &= 3.56\times10^{-8}\text{ per amagat,}\\ \left[T_1(\langle\Delta\sigma\rangle_{\text{av(exp)}})^2\right]_{\text{exp}} &= 3.6(\pm0.4)\times10^{-8}\text{ per amagat.}\end{aligned} \tag{2.2}$$

Torrey admits this calculation is probably fortuitous, and if one considers the order-of-magnitude discrepancy between $\langle\Delta\sigma\rangle_{\text{av(Torrey)}}$ and $\langle\Delta\sigma\rangle_{\text{av(exp)}}$, the theory leads to a two-orders-of-magnitude discrepancy in the theoretical T_1 compared to the experimental T_1. Hunt and Carr use an experimental value for $\Delta\sigma_{\text{av}}$ in Torrey's theory (instead of Torrey's theoretical $\Delta\sigma_{\text{av}}$) and calculate a longitudinal relaxation time that is slightly greater than twice the experimental value for liquid xenon.

Meanwhile, Yen and Norberg, at Washington University of St. Louis, observe a temperature-dependent chemical shift for solid ^{129}Xe presented in the first published work that contains solid xenon NMR data [67]. Specifically, they report self-diffusion coefficients, resonance shifts, and transverse (spin-spin, T_2) relaxation times for a range of pressures (saturated vapor pressures to 20 atm) and temperatures (4–227 K) for naturally abundant xenon in liquid and solid phases. A limiting (lower bound) value of T_1 in a solid is set, $T_1 > 7\times10^3$ s. at 125 K. The main results of the paper concern T_2 values, so paramagnetic impurities such as activated charcoal in glass wool and air are introduced to shorten T_1 to 900 and 600 s, respectively, at 125 K. They mention the impurities did *not* have any effect on T_2. The solid ^{129}Xe T_2 data over a temperature range of 90–160 K matches the Van Vleck rigid-lattice dipolar theory [48] from 90 K to roughly 120 K. Between 120 K up to 160 K, T_2 becomes longer than the rigid-lattice dipolar theory predicts, due to diffusion (motional narrowing).

Assuming a face-centered-cubic (fcc) lattice, a temperature-dependent equation for the diffusion constant D of solid xenon is found,

$$D = 7.4(\pm .3)e^{-7.40(\pm 0.05)\times 10^3/RT}\ \mathrm{cm}^2/\mathrm{s}, \tag{2.3}$$

where R is the molar gas constant and T is temperature. A liquid diffusion coefficient corroborating Hunt and Carr's work is also given, but this result is a factor of two different than a ^{132}Xe radioactive tracer experiment [68]. Yen and Norberg give the resonance shift ΔH (chemical shift) for solid xenon as the linear equation

$$\Delta H = 10.82 - 20.4 \times 10^{-7}\rho H_0, \tag{2.4}$$

where ρ is density and H_0 is the external magnetic field. The term uses a density that relates to the pressure-volume isotherm data presented by the 1963 work of Packard and Swenson [69].

In 1964, Brinkmann (at Rutgers, with Carr) also publishes solid ^{129}Xe resonance-shift data [70]. From this data, it is determined that the density rate-of-change of the chemical shift for solid ^{129}Xe is

$$(\partial \Delta H/\partial \rho)_{\mathrm{solid}} = +(5.3 \pm 0.3)10^{-7} H_0. \tag{2.5}$$

The rate of change is slightly greater than that of liquid, but a *factor of four* smaller than that reported for solid ^{129}Xe by Yen and Norberg ($20.4\times 10^{-7} H_0$) [67]. Following the report of this discrepancy, Lurie et al. (at Rugters) give a theoretical treatment of the local magnetic field shift in solid xenon that, Lurie et al. state, corroborates Brinkmann's data in favor of Yen and Norberg's data [71]. None of the calculated curves fit the entire set of Brinkmann's data, as seen in Fig. 2.1 (see Lurie et al. [71]), but the calculations are much closer to Brinkmann's data than Yen and Norberg's data.

In Lurie et al. [71], the calculation is based on the extension of the diatomic Xe_2 molecule to the solid phase of ^{129}Xe. The assumption behind this pursuit is that the origin of the shift is the same for all phases of xenon. Building on Torrey and Ramsey's work for xenon gas, each of the twelve nearest-neighbor atoms in a fcc xenon lattice is considered a diatomic interaction, ignoring motional correlation between the atoms (the atoms are free to vibrate independently in their lattice position). Summing over the nearest neighbors, the expression for the magnetic-field shift in the solid becomes

$$\begin{aligned}\Delta H(T) &= \sum_{\mathrm{n.n.}} \langle AH \sin^2\theta\ e^{-Z(R-b)}\rangle \\ &= 12AHe^{-Z(R_0(T)-b)}(\sin^2\theta)_0\langle n|1 + \frac{Z^2u_z^2}{2} + \frac{Z(u_x^2+u_y^2)}{2R_0}|n\rangle\end{aligned} \tag{2.6}$$

where A, Z, and b are parameters, with A representing a sort of interaction strength. H is the applied field, R is the separation between two atoms, θ is the angle between R and H, R_0 is the equilibrium separation between two atoms, $\mathbf{u}$ is the displacement from equilibrium, $(\sin^2\theta)_0 = 2/3$ is the equilibrium average of $\sin^2\theta$ over the fcc

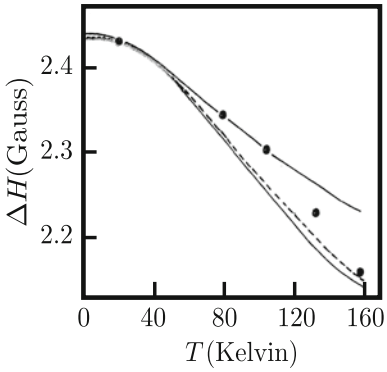

Fig. 2.1 A comparison of experimental and theoretical values of the chemical shift in solid ^{129}Xe is shown. The bold circles are Brinkmann and Carr's data [70, 72]. The lower solid curve is computed from the Lennard-Jones 13-6 potential using $A = 1.180 \times 10^{-4}$. The upper solid curve is computed using a Buckingham 13-6 potential and Adrian's calculated value of A, $A = 7.82 \times 10^{-5}$ [73]. The dashed curve is computed using the Lennard-Jones 13-6 potential and the value $A = 1.07 \times 10^{-4}$. All data and calculated values are normalized to agree at 21 K and correspond to a field of 7100 G. (See [71])

lattice, and the brackets, along with the symbol $\langle n| \, |n\rangle$, represent an average over the canonical ensemble. The value for parameter $Z = 2.506\,\text{Å}^{-1}$ is taken from Adrian's 1964 work [73]. Various methods of obtaining values for A (and the dependent b) are used, including data from Brinkmann and Carr's complimentary 1966 work [72], dilute gas shift data of the Rutgers group, or the value presented in Adrian's work. The value of A obtained from the Washington data is deemed implausible because it is not close enough to the liquid value of A (the Washington and Rutgers value of A in liquid xenon agree). For the canonical calculation, various potentials are used, including Lennard-Jones 13-6,

$$\phi_\epsilon(R) = \frac{6 \times 13 \times \epsilon}{7} \left[\frac{1}{13} \left(\frac{R_0}{R} \right)^{13} - \frac{1}{6} \left(\frac{R_0}{R} \right)^{6} \right], \tag{2.7}$$

and a Buckingham potential,

$$\phi_\epsilon(R) = \frac{6 \times 13 \times \epsilon}{7} \left[\frac{1}{13} \exp\left(\frac{-13(R - R_0)}{R_0} \right) - \frac{1}{6} \left(\frac{R_0}{R} \right)^{6} \right], \tag{2.8}$$

and a standard Lennard-Jones 12-6 potential. All variations of potentials and plausible A values fit with the Rutgers data better than the Washington University data.

Also in 1966, Warren and Norberg (at Washington University) study relaxation and chemical shifts in ^{131}Xe due to the nuclear quadrupole moment in the spin-3/2 nuclei [74]. The quadrupolar relaxation theory used to describe the data is that of Van Kranendonk's for a solid with a Debye phonon spectrum [75]. Specifically, substituting the quadrupole moment for the dipole moment in the Waller theory of

dipolar relaxation [31, 76], a theory is developed that uses the quadrupole-phonon interaction as an explanation of the data. The direct-phonon process (one phonon) is discounted as negligible and the focus is on the quadratic or "Raman" term—the term that corresponds to absorption and emission of phonons whose frequency difference is at the Larmor frequency ω_0, or $2\omega_0$. A first principles calculation of the overlap, or van der Waals interactions (used to calculate the strength of the time-dependent electric-field gradients) is compared to the experimental T_1 at 100 K,

$$T_{1(\text{theory})} = 1.3 \text{ s}, \quad T_{1(\text{exp})} = 0.70 \pm 0.05 \text{ s}. \tag{2.9}$$

Therefore, the theory requires half of the interaction strength to account for the data at 100 K. The other test of the theory is the temperature dependence. Notice the distinction, while the theory should presumably account for both the strength of the relaxation interaction and the temperature dependence, it is possible to claim ignorance of the exact strength of the relaxation and obtain the strength from the observed T_1 *itself*, and separately test the predicted temperature dependence of T_1. By normalizing the interaction strength to experimental T_1 data taken at 77 K, the temperature dependence of the theory for quadrupole relaxation via the two-phonon Raman process is shown to account for the experimental ^{131}Xe data in the range of 9–110 K. A temperature-dependent Deybe temperature provided by Packard and Swenson [69] is used to correct the theory for temperatures above 110 K to the melting point of xenon. In all, the first principles calculation of the quadrupole relaxation via the two-phonon Raman process has the same temperature dependence, but the calculation for the interaction strength is inaccurate. This is expected because it is difficult to determine the potential of xenon in a lattice; the gaseous xenon potential also remains not well known. Chemical-shift data for solid ^{131}Xe is also given, and the value extrapolated,

$$-\frac{1}{H_0}\frac{\partial(\Delta H)}{\partial \rho} = (18.2 \pm 1.1) \times 10^{-7} \text{Å}^{-1}, \tag{2.10}$$

matches closely with Yen and Norberg's chemical shift data for ^{129}Xe.

In 1967, Warren and Norberg present an extensive study of T_2 for solid ^{129}Xe and ^{131}Xe [77]. A second moment (and in turn T_2) for ^{129}Xe is found that is approximately the same as the theoretical second moment found with Van Vleck's theory of dipolar broadening in a rigid lattice [48]. At a lower magnetic field, this experiment reaffirmed the same T_2 of that reported by Yen and Norberg [67].

Finally, to end this first wave of NMR studies of solid xenon, there is another set of solid xenon NMR data, published in 1972 by Cowgill and Norberg at Washington University in St. Louis [78]. The relative chemical shift in solid ^{131}Xe is found to be

$$-\frac{1}{H_0}\frac{\partial(\Delta H)}{\partial \rho} = (5.72 \pm 0.36) \times 10^{-7} \text{Å}^{-1}. \tag{2.11}$$

In this paper, they mention that they are not able to reproduce the larger shifts previously reported in solid xenon by Yen, Warren, and Norberg. This result corroborates

Brinkmann and Carr's data [72] and the theoretical work provided by Lurie et al. [71], and is an order of magnitude less than the data provided by Yen and Norberg [67].

With this, there is a break in the literature for solid ^{129}Xe NMR for roughly 20 years. The early results proved to be fairly volatile, with pure theory never exactly describing the data. Trends, such as similar temperature dependence, suggest that the quadrupolar-relaxation mechanism mediated by the Raman-scattering of phonons accounts for ^{131}Xe experimental data. Certain experimental results, such as the chemical shift data, remain unexplained at the end of the first wave of papers. In this brief history, it is seen exactly how reproducibility and theoretical determination is a significant problem when concerning solid xenon.

2.2.2 *Reincarnation via Hyperpolarization*

The early work has a lack of solid ^{129}Xe longitudinal relaxation data without impurities such as oxygen. This deficiency comes from a practical problem—for conventional solid NMR measurements, the relaxation times are too long for ^{129}Xe for an extensive study to be worthwhile; all of the experiments in the early work monitored thermal polarization and, with T_1 times for ^{129}Xe reaching upwards of hours, a T_1 measurement was presumably determined too long to be practical. "Conventional," in this sense, describes experiments of the saturation-recovery type, as very high fields, low temperatures, or very large amounts of xenon would be required to observe relaxation for solid ^{129}Xe in thermal equilibrium. Another problem plaguing the early work was that of impure samples. Oxygen has a detrimental effect on a reliable T_1 measurement. As mentioned in Sect. 2.2.1, oxygen was purposefully introduced to cut T_1 times by orders of magnitude so that T_2 measurements were feasible.

Hyperpolarization of ^{129}Xe provides the ability to run T_1 experiments in a beneficially different way. Starting with a very large polarization in the ^{129}Xe, created by hyperpolarization via spin exchange with optically pumped Rb atoms (see Appendix C), it is possible to monitor polarization loss as the ^{129}Xe returns to thermal polarization. Using pulsed NMR, the large polarizations afforded by hyperpolarization techniques lead to a very large signal with very small flip angles. The small flip angles lead to minimal polarization being sacrificed for the actual process of measuring relative polarization loss. Therefore, the time required to measure T_1 in a particular sample only needs to be long enough to reliably trace out the polarization decay curve (a rule of thumb is the time of measurement must be past T_1). This method drastically reduces the run time of the experiment, when compared to methods that start from thermal polarization of the sample. With thermal polarization measurements, large flip angles and perhaps averaging are needed to see a sufficient pulsed-NMR signal of ^{129}Xe at higher temperatures. A large flip angle means the method of finding T_1 is limited to typical T_1 NMR measurement techniques: inversion recovery, saturation recovery, etc. [31, 32, 79]. In each of these conventional NMR techniques, the first step is (typically) to wait many times T_1 so that the sample

has maximum thermal polarization. Therefore, *one* data point to map out the characteristic T_1 curve takes multiples of T_1. T_1 measurements using hyperpolarization techniques typically record 50–150 points over the course of one experiment; to get the same resolution using thermal polarization techniques, the time required is

$$\begin{aligned}\text{Thermal Polarization Run Time} &= (\text{Time per data point}) * (\text{Data points}) \\ &= (4(\pm 1)T_1) * (100 \pm 50) = (400 \pm 200) * T_1.\end{aligned} \tag{2.12}$$

For ^{129}Xe, a T_1 of 2–3 h at 77 K would lead to a thermal polarization experimental run time of, at minimum, weeks in order to achieve the same resolution as a hyperpolarized sample does in hours. This back-of-the-envelope calculation clearly shows that hyperpolarization gives quite an experimental advantage over thermal polarization for studying systems with extremely long T_1 times.

2.2.3 Review of Hyperpolarized ^{129}Xe Experimental Results

In 1990, Cates et al. (at Princeton) report the first-ever hyperpolarized solid ^{129}Xe NMR signals [80]. Therein, the Rb in a Xe-Rb borosilicate-glass cell is optically pumped using 0.5–5 W of circularly polarized light at the D_1 transition (795 nm). The ^{129}Xe nuclei are polarized in spin-exchange collisions with the polarized Rb atoms, after which the cell is bathed in liquid nitrogen at 77 K. After crystal formation, the cell is brought to various temperatures: 77, 87, and 100–145 K. A range of magnetic field values are also used, from 0 to 1800 Gauss. Two different classes of cells are investigated; cells with high pressures (5 atm) of ^{129}Xe and cells with low pressures (1 atm) of ^{129}Xe. In addition, two different types of xenon are used: naturally abundant xenon and enriched xenon (72.9 % ^{129}Xe, 5.3 % ^{131}Xe). The NMR is conducted with adiabatic fast passage to monitor polarization of the sample [31]. In this work, a difference in T_1 is found that depends on the room-temperature gas pressure of the cell. Interestingly, for the low-pressure cell of enriched xenon, $T_1 = 128.33 \pm 5$ min, and for the high-pressure cell, $T_1 = 163.33 \pm 10$ min. (As shown in Sect. 2.4, perhaps a cell with an insufficient partial pressure of xenon is not able to pass through the liquid phase, and leads to different crystal structures.) The relaxation time for the high-pressure cell of naturally abundant xenon is reported as $T_1 = 141.66 \pm 16.66$ min. All other obtained solid ^{129}Xe T_1 values are plotted in two figures contained in the paper and a compilation of values is also listed in Michael Gatzke's dissertation [81]; values relevant to this thesis are plotted in Fig. 2.2. A calculation by Abragam and Goldman gives a relaxation rate due to very small concentrations ($N_S/N_I \ll 1$) of impurities in a lattice [85],

$$\frac{1}{T_1} = \frac{8\pi}{5}\frac{S(S+1)}{3}\frac{N_S}{N_I}(\gamma_S\gamma_I)(\Delta H_n)^2\frac{T_{1e}}{1+(\gamma_I H_0 T_{1e})^2} \propto N_I. \tag{2.13}$$

Here, N_S and N_I are, respectively, the number densities of the paramagnetic impurities and spin-1/2 xenon nuclei, γ_S and γ_I are, respectively, the gyromagnetic ratios

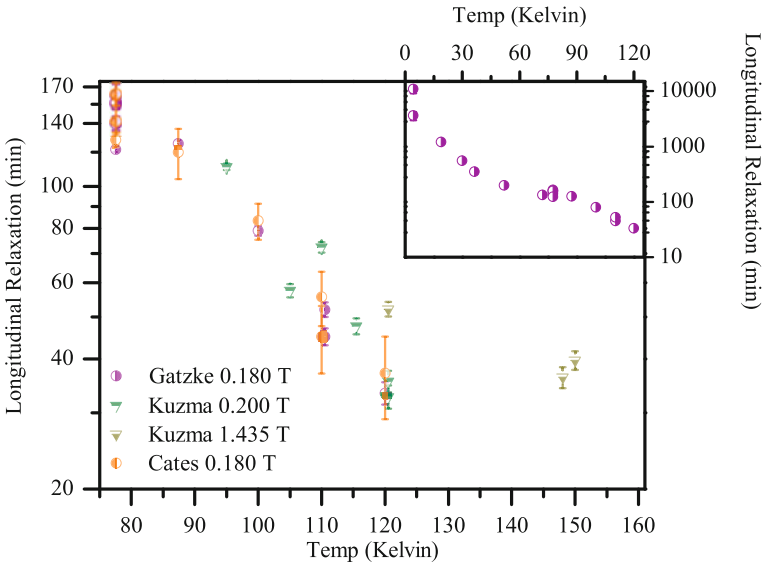

Fig. 2.2 A compilation of temperature-dependent solid ^{129}Xe T_1 values is shown. Data is taken from [80–84] at listed magnetic field values is shown. Higher temperature data at low field values are shorter than 20 min due to the onset of vacancy diffusion relaxation, and therefore left out of plot. *Inset* Extended temperature range of solid ^{129}Xe T_1 times from [81, 82]

for the paramagnetic impurity and ^{129}Xe, $\Delta H_n \approx \gamma_I \hbar N_I$ is the nuclear linewidth due to spin-spin interactions in the rigid lattice, T_{1e} is the relaxation of the electronic spin S, and H_0 is the external magnetic field. Therefore, if paramagnetic impurities are causing the relaxation, enriched xenon would have a relaxation rate that is a factor of 72.9 %/26 % higher than that of natural xenon. However, the data show no discernible dependence on isotopic concentration of ^{129}Xe. Also, the amount of Rb in the xenon lattice required with this analysis would exceed the relative concentration of Rb atoms at room temperature before freezing the xenon, furthering the evidence against this mechanism of relaxation. The Rb also serves as a "getter" for any oxygen that may be in the cell, so paramagnetic relaxation caused from O_2 is also discounted. Above 120 K, natural xenon shows a slower relaxation rate than enriched xenon, indicating a dipolar-dipolar type relaxation mechanism that is caused by the onset of hopping (this also leads to motional narrowing in the NMR lineshape). The spin-rotation interaction mediated by Raman-phonon scattering is suggested as a possible relaxation mechanism below 120 K; this mechanism gives roughly the same T^2 temperature dependence as the 77–120 K data.

A few things are unclear from Cates et al. [80] as a singular work; one is the calculation of the spin-phonon coupling, the other is at what magnetic field the temperature-dependent data is taken. The relaxation rate $1/T_1$ is suggested to be dominated by Raman scattering of phonons by the nuclear spin-rotation interaction

$$V_I = \gamma_I \mathbf{I} \cdot \mathbf{N}. \tag{2.14}$$

Here, γ_I is now labeled as the *coupling coefficient* (not gyromagetic ratio), **N** is the rotational angular momentum of a ^{129}Xe atom around any other xenon atom, and **I** is the spin angular momentum of the ^{129}Xe nucleus. The coupling coefficient used is

$$\gamma_I \approx nA\gamma_S/E_e, \tag{2.15}$$

where n is the effective number of outer-shell electrons involved in the interaction, $A/h \approx 10^{10}$ Hz is the mean magnitude of the hyperfine interaction between a ^{129}Xe nucleus and one of the n electrons, and $E_e \approx 10$ eV is the energy required to excite one of the n electrons. The value of γ_S is here defined as the coupling constant in the spin-rotation interaction $V_S = \gamma_S \mathbf{N} \cdot \mathbf{S}$ between the spin of a Rb atom moving with rotational angular momentum **N** about a Xe atom. The data are best fitted with a coupling coefficient of $\gamma_I \approx 35$ Hz, but it is unclear why this is, or how the fit is actually accomplished. Presumably the given equation

$$1/T_1 = aT^2 + be^{-E_D/kT}, \tag{2.16}$$

is used in the fitting process, but a relation between the parameter a and the coupling coefficient γ_I is not given. A previously measured value of $\gamma_S/h = 1.6$ MHz [86] is used to estimate how many electrons take place ($n \approx 7$) in the interaction from the approximation in Eq. 2.15. Temperature-dependent data are given, but a magnetic field value is not given for the measurement (though this is clarified in Gatzke's thesis, $H_0 = 1800$ G [81]).

An extension to the temperature-dependent T_1 of solid ^{129}Xe is presented by Gatzke et al., in 1993 [82]. In the article, they attempt to reaffirm that the spin-rotation interaction is the dominating relaxation mechanism from 20 to 120 K. A more in-depth analysis is given, using chemical-shift measurements to derive a value for the spin-rotation coupling constant

$$\frac{\gamma_I}{h} = \left(\frac{\mu_I}{I\mu_B}\right)\left(\frac{\hbar}{8\pi Mr_0^2}\right)(\sigma_s - \sigma_g) = -27 \text{ Hz}. \tag{2.17}$$

Here, μ_I is the magnetic moment of ^{129}Xe, μ_B is the Bohr magneton, M is the average mass of a xenon atom, and $r_0 \simeq 4.4$ Å is the equilibrium internuclear separation. Raftery et al., give a chemical shift in solid ^{129}Xe at 77 K of $(\sigma_s - \sigma_g) = 317$ parts per million (ppm) from that of gaseous ^{129}Xe [87, 88]. The estimated coupling strength is used in the relaxation calculation (for the spin-rotation interaction mediated by a Raman-scattering process), giving the approximate expression (well-approximated to better than 2 %[1])

$$\frac{1}{T_1} \simeq 8.20 \times 10^4 \left(\frac{\gamma_I}{h}\right)^2 \left(\frac{h}{kT_D}\right)\left(1 + \frac{2}{3}\epsilon + 0.122\epsilon^2\right)(T^*)^9 \int_0^{1/T^*} \frac{e^x x^8}{(e^x - 1)^2} dx. \tag{2.18}$$

[1] It is unclear what 2 % means from the paper in this context.

http://www.springer.com/978-3-319-13631-8

129 Xe Relaxation and Rabi Oscillations

Limes, M.

2015, XXI, 136 p. 42 illus., 33 illus. in color., Hardcover
ISBN: 978-3-319-13631-8